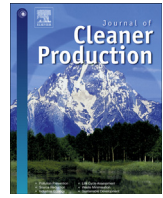




Contents lists available at ScienceDirect

Journal of Cleaner Production

journal homepage: www.elsevier.com/locate/jclepro

Impact of un-deformed chip thickness on specific energy in mechanical machining processes



Vincent A. Balogun*, Paul T. Mativenga

School of Mechanical, Aerospace and Civil Engineering, The University of Manchester, Manchester M13 9PL, United Kingdom

ARTICLE INFO

Article history:

Received 12 August 2013

Received in revised form

7 January 2014

Accepted 11 January 2014

Available online 22 January 2014

Keywords:

Specific cutting energy coefficient

Un-deformed chip thickness

Manufacturing sustainability

ABSTRACT

Energy demand reduction is a grand challenge for manufacturing sustainability in order to reduce the escalating cost of energy and to cut down on the carbon footprint of manufacturing processes. The direct electrical energy requirements in manufacturing and machining in particular can be modelled from the basic energy required by the machine tool and the energy for actual material removal (tip energy). However, energy centric modelling of manufacturing processes is in its infancy and related material processing data is limited and of low integrity. It has often been assumed that the specific cutting energy is a constant value for particular workpiece materials. This paper is inspired by the mechanistic force modelling and the size effect phenomenon in machining. The aim of this work was to investigate the specific electrical energy demand in machining and model its relationship to thickness of material removed. To this end, specific energy evaluated in cutting tests was empirically modelled. This work is comprehensive in that it covers a wide range of un-deformed chip thickness as well as three workpiece materials. A new and fundamental understanding of the variation of specific energy with chip thickness is reported for the first time. This can be an evidence base for a generic model for the dependence of specific energy on un-deformed chip thickness. This information is vitally important to raise the integrity of energy labelling of machining processes and as a backbone to process optimisation in order to reduce electrical energy demand and promote manufacturing sustainability.

© 2014 Elsevier Ltd. All rights reserved.

1. Introduction

Reducing electricity consumption and CO₂ emission is the driving force for optimising energy demand in manufacturing industry. This addresses the objectives of manufacturing sustainability and resource efficiency. Optimisation of direct electrical energy consumption and improving the energy efficiency of mechanical machining processes is influenced by material characteristics and process parameters. The fundamental approach to modelling energy in manufacturing processes is based on the 'Basic' energy state and 'Tip' energy (Dahmus and Gutowski, 2004). This has been extended recently to include the 'Ready' energy state (Balogun and Mativenga, 2013). These states are described by others as start-up, idle and cutting states (Hu et al., 2012). For a manufacturing process, energy is required to start the production equipment or resource (Basic energy), to prepare the process for value adding activity (Ready State) and finally for actual manufacturing for example 'Tip' energy in machining. The tip energy is the energy demand at the cutting tool tip (cutting edge) and

represents the energy for actual material removal. A fundamental energy demand model was proposed by Gutowski et al. (2006), as in Equation (1).

$$E = (P_0 + k\dot{v})t \quad (1)$$

where, E represents the total energy demand by the manufacturing process in J , P_0 is the power in W demanded by the production equipment in this case the machine tool when operating at zero load, t is the production time in s , \dot{v} is the rate of material processing in $\text{mm}^3 \text{ s}^{-1}$ and k is specific cutting energy in W s mm^{-3} .

Gutowski's et al. (2006), energy model presented above is in synergy with 'The Cooperative Effort in Process Emission' (CO2PE!) (Kellens et al., 2012) approach. The aim of the CO2PE! methodology was to standardise energy reporting and data collection in manufacturing processes. This initiated a more unified and globally compatible classification of energy consuming machines in the manufacturing sector. In the CO2PE! methodology, machine tool states was classified into two categories: 'Basic State' and 'Cutting State'. These classifications are aimed to define and report, on a global scale, how energy consumption in machine tools is distributed.

* Corresponding author.

E-mail address: vincent.balogun@manchester.ac.uk (V.A. Balogun).

Few researchers for example Lin et al. (2013), investigated the specific cutting energy of a unit process and presented energy models as shown in Table 1 and Equations (2)–(5). Also, Qiulian et al. (2013) reported that the specific energy can be used as a measure of energy efficiency in manufacturing. These approaches normalised the total energy consumption in machining to the volume of material removed. These approaches do not disaggregate energy consumption into the standardised framework as proposed by CO2PE! and as implied by Equation (1). Thus, there still exists a knowledge gap with regards characterising and modelling the specific tip energy requirements in machining. This vital information will enable consideration of differences in workpiece material when modelling and selecting optimum cutting conditions for minimum energy demand in machining.

For process level energy efficient machining to be achieved, an understanding of the influence of material characteristics and process variables on the specific cutting energy coefficient is necessary. Process planners have to select optimum process variables for achieving manufacturing sustainability and energy efficient machining in particular (Rajemi et al., 2010). Inappropriate selection of cutting variables can hinder energy savings. For example, selection of cutting conditions can lead to significantly higher specific cutting energy in grinding operations (Boothroyd and Knight, 1989). Moreover, specific cutting energy is an important parameter which is directly related to chip morphology, cutting forces, tool wear and machined surface integrity (Pawade et al., 2009). Kuram et al. (2013), related specific energy values to cutting fluid effectiveness, tool wear and machined components surface roughness.

1.1. The wider importance of specific energy data

The specific cutting energy varies for different machining processes even when the workpiece material properties remain the same. For example, the specific cutting energy for grinding operations is higher compared to other machining processes like turning and milling. This is due to the inefficient nature of the abrasive grit in cutting compared to the use of defined cutting edges as in other mechanical machining processes. This knowledge of specific energy can be important because for example, the specific cutting energy in grinding operations influence surface integrity of machined components (Paul and Chattopadhyay, 1995). The specific energy can also be linked to the process mechanisms. Ghosh et al. (2008), reported that chip formation, ploughing, primary and secondary rubbing phenomenon are major factors affecting the

surface integrity in grinding. Polini and Turchetta (2004), presented a model for the specific energy in stone grinding. In their analysis, it was shown that, the specific energy is related to the equivalent chip thickness by a power function. The specific energy range for grinding stone was shown to decrease with the increase of the equivalent chip thickness from a maximum of 25 kJ/mm³ at 200 mm/min to 6 kJ/mm³ at 600 mm/min.

Workpiece surface integrity (Guo et al., 2012) has been correlated to specific cutting energy for 'High Speed Machining' conditions. The cutting edge angle (Lucca et al., 1993), swept angle (Bayoumi et al., 1994), rake angle and other cutting tool geometries have distinct influences on the specific cutting energy. Burr formation has also been reported as linked to higher specific cutting energy. In their analysis with AISI 1045, Zhang et al. (2012, 2013), reported that "Poisson burr" height increases when the ratio of undeformed chip thickness to the cutting edge radius is less than 1. This result implies that higher specific cutting energy can be associated with larger burr size and this can be an important attribute for process monitoring.

1.2. Size effect in machining

In milling, chip formation does not only depend on material characteristic and cutting tool geometry, but also on the ratio of the feed per tooth to the cutting edge radius. For example, in machining, the minimum chip thickness is the ratio of feed per tooth to cutting tool edge radius below which no chips are formed. This is the lower limit for machining. The minimum chip thickness has been reported to be in the range of ratio of un-deformed chip thickness to cutting edge radius of 0.2–0.4 (Aramcharoen and Mativenga, 2009). At a value below the minimum chip thickness the process is dominated by high frictional force due to rubbing and plastic deformation. If the ratio of un-deformed chip thickness to the cutting edge radius is less than 1, the dominance of the size effect phenomenon increases and rubbing and ploughing is associated with size effect in machining (Bissacco et al., 2006). This phenomenon increases the specific cutting forces (Ducobu et al., 2009). Filiz et al. (2007), reported that the size effect induces a nonlinear increase in specific cutting force. The concept of a nonlinear variation of specific cutting force or pressure has been the backbone of empirical force modelling in machining. Table 2 shows other specific cutting pressure models as documented in literature.

It is clear from the review above that a number of researchers over the years have modelled the specific cutting force and specific cutting pressure through the measurement and estimation of force component and the material removal rate. Others attributed the

Table 1

Global specific energy models found in literature combining both basic and tip energy.

| Authors | Specific energy model |
|--------------------------|---|
| Draganescu et al. (2003) | $E_{cs} = \frac{P_c}{60\eta Z}$ (2) |
| Li and Kara (2011) | $SEC = C_0 + \frac{C_1}{MRR}$ (3) |
| Diaz et al. (2011) | $e_{cut} = k^* \frac{1}{MRR} + b$ (4) |
| Lin et al. (2013) | $SEC = k_0 + k_1 \frac{n}{MRR} + k_2 \frac{1}{MRR}$ (5) |

Where E_{cs} , SEC , e_{cut} represents specific energy consumption, P_c is the cutting power, η is machine tool efficiency, C_0 and C_1 are empirical coefficients, Z and MRR represents the material removal rate, k is a constant and has units of power and b represents the steady-state specific energy, k_0 is the specific energy requirement in cutting operations, k_1 is the specific coefficients of spindle motor, k_2 is the constant coefficient of machine tools and n is the spindle speed in rev/s.

Table 2

Models of specific cutting pressure.

| Author(s) | Specific cutting pressure model |
|-----------------------------|-----------------------------------|
| Kronenberg (1927) | $K_s = Ct^{-a}s^{-h}$ (6) |
| Schroder (1934) | $K_s = \alpha + \beta h^{-1}$ (7) |
| Kienzle (1952) | $K_s = Ks_{1.1} + h^{-x}$ (8) |
| Hucks ¹ , (1955) | $K_s = C_1 q^{-0.25}$ (9) |
| Hucks ² , (1955) | $K_s = A(1 + Bh^{-1})$ (10) |
| Sabberwal (1962) | $K_s = Ch^x$ (11) |

Where K_s represent the specific cutting pressure, C , α , β , K , C_1 , A , B , a and x are constants depending upon the workpiece material and cutting tool geometry, t , is the depth of cut, h is the chip thickness at any instant, s is the feed per tooth and q is the area at any instant.

specific cutting force trend to the size effect in machining. Chip thickness, machining mechanisms and the so called “size effect” should influence the magnitude of the specific energy required in machining.

2. Aim and objective

The aim of this work was to investigate the specific electrical energy requirement in machining and its relationship to thickness of material removed and “size effect” and improve the integrity of data for specific cutting energy coefficients. The methodology was to undertake cutting tests at set values of un-deformed chip thickness and evaluate the specific energy coefficient. During the cutting tests, electrical current demand was measured and the variation of power requirement for different material removal rate was evaluated and the gradient used as a measure of the specific energy requirement. This was achieved through the direct measurement of the electrical energy consumption by varying the un-deformed chip thickness at different process parameter levels, cutting tool geometry and swept angles. This work will contribute towards the development of a realistic and robust model for estimating the specific cutting energy coefficient, and provide valuable data for resource efficient machining in particular energy centric production planning.

3. Modelling and experimental setup

3.1. Research methodology

Cutting tests were planned to assess the effect of chip thickness on the specific energy demand in machining. The idea was to undertake cutting tests in single tooth milling mode and at the same time measure the current drawn by the machine. This enables tracing the impact of chip thickness. The electrical current was then used as basis for calculating the power demand. If power demand is considered with machining time, then area under the power–time curve is the energy consumed. When the cutting tests are done at different material removal rates, the plot of power demand versus material removal rate has a gradient equal to the specific cutting energy in $W s mm^{-3}$. The specific cutting energy was evaluated at a defined chip thickness and for a number of chip thicknesses and the variation of the specific cutting energy with chip thickness was characterised.

3.2. Cutting test details

Machining trials were conducted on a Mikron HSM 400 machining centre. This machine has a HVC140-SB-10-15/42-3FHSK-E40 spindle and Heidenhain TNC 410 NC controller. The investigation was done for three different materials shown in Table 3. The chemical composition and cutting parameters of the

Table 4
Cutting tool geometry.

| Geometry | Values |
|---|--------|
| Nose radius (mm) | 0.4 |
| Edge radius (μm) | 60 |
| Rake angle (deg.) | +5 |
| Rake face primary chip breaker land (μm) | 60 |
| Clearance angle (deg.) | 7 |

three different workpiece materials are provided in Table 3. The materials selected for investigation were aluminium AW6082-T6 alloy, AISI 1045 steel alloy, and titanium 6Al-4V alloy. The workpiece materials were selected to represent the major applicable engineering material classes. The cutting speeds used were derived from cutting tool manufacturers recommendations. The depth of cut was determined by the thickness of the workpiece material and the feedrates were selected to overlap the process window. The radial width of cut was varied to create different material removal rate. This parameter has a low influence on basic energy and hence is beneficial to vary when investigating tip energy.

During the machining process, cutting was undertaken on the straight cutting edge by avoiding engaging the nose radius in side milling. The set up was near-orthogonal machining. A single insert was used and the conditions were such that the maximum number of cutting edges engaged at any instance was 1. This ensured that the variation of power requirement could be related to the chip thickness. The investigations covered seven different feedrates (un-deformed chip thickness). As mentioned before, at each feedrate, the material removal rate was varied by machining at four different radial width of cut. Each experimental run was repeated three times.

A tool holder E90X-D08-C10-06 with an overhang of 25 mm was used. The holder was mounted with a single insert, SOMT-060204-HQ and used for an end milling operation in order to mimic orthogonal cutting. The insert was a general purpose TiAlN coated carbide insert with geometry shown in Table 4. This was used for milling the three selected materials to enable adequate comparison and standardisation between the different materials. The machining trials were conducted under a dry cutting environment in order not to mask the differences brought by workpiece materials.

Each workpiece material was 100 mm \times 50 mm \times 3.5 mm. The material was held in a vice with a protrusion of 12 mm, just enough to accommodate a set of machining trials. This was done in order to reduce the workpiece and cutting tool vibrations to the barest minimum. The length of cut was 50 mm. Each experimental trial was repeated three times. A new cutting tool edge was used in order to minimise the effect of tool wear. The electrical current consumption during the machining process was measured with a FLUKE 345 Power Clamp meter.

Table 3
Cutting parameters for milling trials.

| | Aluminium AW6082-T6 alloy | AISI 1045 steel alloy | Titanium 6Al-4V alloy |
|-----------------------------|--|---|--|
| Feed (mm/tooth) | 0.01–0.55 | 0.01–0.55 | 0.01–0.55 |
| Depth of cut (mm) | 3.5 | 3.5 | 3.5 |
| Cutting velocity (m/min) | 210 | 156 | 80 |
| Radial width of cut (mm) | 0.25–1.00 | 0.25–1.00 | 0.25–1.00 |
| Tool diameter (mm) | 8 | 8 | 8 |
| Chemical composition (Max) | 1%Mn, 0.5%Fe, 1.2%Mg, 1.3%Si, 0.1%Cu, 0.2%Zn, 0.1%Ti, 0.25%Cr, Balance Al. | 0.46%C, 0.40%Si, 0.65%Mn, 0.40%Cr, 0.10 Mo, 0.40%Ni, 0.63% Others | 89.37%Ti, 6%Al, 4%V, 0.08%C, 0.3%Fe, 0.2%O ₂ , 0.05%N |
| Workpiece material hardness | HV 104.5 | HV 238.2 | HV 353.2 |

Table 5
Taguchi L9 experimental design and responses.

| Cutting velocity, v_c (m/min) | Feed per tooth, f_z (mm/tooth) | Depth of cut, a_p (mm) | Width of cut, a_e (mm) | Material removal rate, Q (mm ³ /s) | Power (W) |
|---------------------------------|----------------------------------|--------------------------|--------------------------|---|-----------|
| 100 | 0.1 | 0.5 | 0.6 | 1.33 | 3054.90 |
| 100 | 0.2 | 1.0 | 0.8 | 7.07 | 3074.07 |
| 100 | 0.3 | 1.5 | 1.0 | 19.89 | 3090.13 |
| 120 | 0.1 | 1.0 | 1.0 | 5.30 | 3113.68 |
| 120 | 0.2 | 1.5 | 0.6 | 9.55 | 3135.28 |
| 120 | 0.3 | 0.5 | 0.8 | 6.37 | 3164.69 |
| 150 | 0.1 | 1.5 | 0.8 | 7.96 | 3101.11 |
| 150 | 0.2 | 0.5 | 1.0 | 6.63 | 3084.31 |
| 150 | 0.3 | 1.0 | 0.6 | 11.94 | 3083.66 |

3.3. Influence of varying cutting parameters on power demand during mechanical machining processes

In machining, there is the need to understand the dominant parameters that influences the specific energy. This information is useful in developing process control strategies for reducing energy demand of different workpiece materials. A pilot test was therefore carried out to study the influence of process variables on power demand during machining process. A dry milling operation was conducted on the Mikron HSM 400 with single inserts of code SOMT-060204-HQ on AISI 1045 steel. The process variables investigated were cutting velocity v_c , feed f_z , depth of cut a_p and radial depth of cut a_e . The experimental design was an L9 Taguchi orthogonal array. The results were analyzed on Minitab 16 software to access the effects of varying cutting parameters that influence the power consumption in machining AISI 1045 steel. The experimental design and responses were as shown in Table 5.

Fig. 1 shows the main effects plot for power demand in machining. Using the minimum the better objective, the highest point on the signal to noise ratio curve is the set of cutting conditions which lead to minimum power requirements. Therefore, Fig. 1 shows that in order to minimise power demand, a low cutting

velocity of 100 m/min, low feedrate of 0.1 mm/tooth, mid-range depth of cut of 1.0 mm and a low radial width of cut of 0.6 mm must be selected. In Fig. 1, the variable with the largest signal-to-noise ratio gradient is the dominant parameter. Therefore, it is evident that the cutting velocity is the dominant parameter as supported by Table 6. This is well accepted because in machining the machine tool 'Basic' energy state dominates power demand and a major component of this is the spindle.

From the results it can be inferred that varying either the depth of cut a_p , and/or radial width of cut a_e , will have a lower impact on the power demand in mechanical machining compared to changing cutting velocity or spindle speeds. The second most important factor is the feed per tooth which drives the size effect in machining. Hence, in the subsequent study and machining cuts to evaluate specific energy, the cutting velocity V_c , was kept constant so that its dominant effect would not mask the modelling impact of feed per tooth (chip thickness). The axial depth of cut was fixed by the thickness of the material hence the radial width of cut was varied between 0.25 mm and 1.00 mm in order that different material removal rates could be computed and power demand measured. This enabled power and material removal rate to be plotted and specific cutting energy coefficient evaluated.

4. Results and discussions

After milling on the Mikron HSM 400 high speed milling centre the power demand was calculated from the measured current and the material removal rate Q for each set of experiment was plotted against the power demand. The slope of each graph represents the specific cutting energy coefficient in $W s mm^{-3}$ for the selected workpiece material at the defined cutting conditions. This is in accordance with the modelling approach introduced by Gutowski et al. (2006), in Equation (1) where the basic energy is modelled separately from the tool tip energy. As mentioned earlier, this approach also supports the EU based COP2E! (Kellens et al., 2012). Fig. 2a,b and c shows the variation of power demand in machining

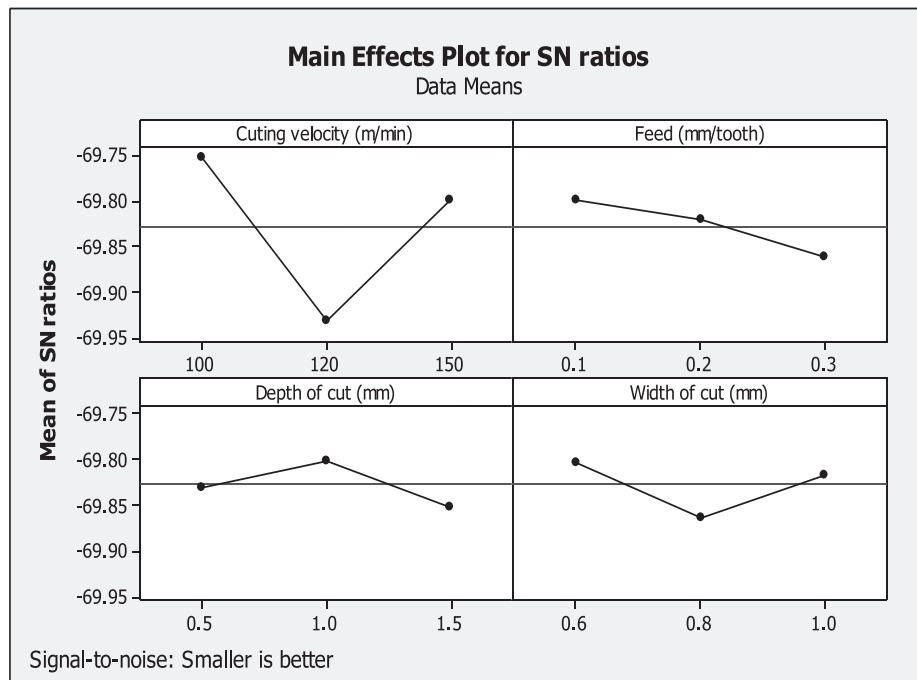


Fig. 1. Key Process variable ranking for power demand in machining of AISI 1045 steel alloy.

Table 6
Effect ranking based on Minitab 16 analysis.

| Level | V_c (m/min) | f_z (mm/tooth) | a_p (mm) | a_e (mm) |
|-------|---------------|------------------|------------|------------|
| 1 | 3073 | 3090 | 3101 | 3091 |
| 2 | 3138 | 3098 | 3090 | 3113 |
| 3 | 3090 | 3113 | 3109 | 3096 |
| Delta | 65 | 23 | 18 | 22 |
| Rank | 1 | 2 | 4 | 3 |

with material removal rate for cutting aluminium AW6082-T6 alloy, AISI 1045 steel alloy and titanium 6Al-4V alloy respectively at a feed f_z of 0.01 mm/tooth. It is observed from Fig. 2a,b and c that at the lowest feed of 0.01 mm/tooth, the specific cutting energy as represented by the slope of the graph was 13.08, 5.38 and

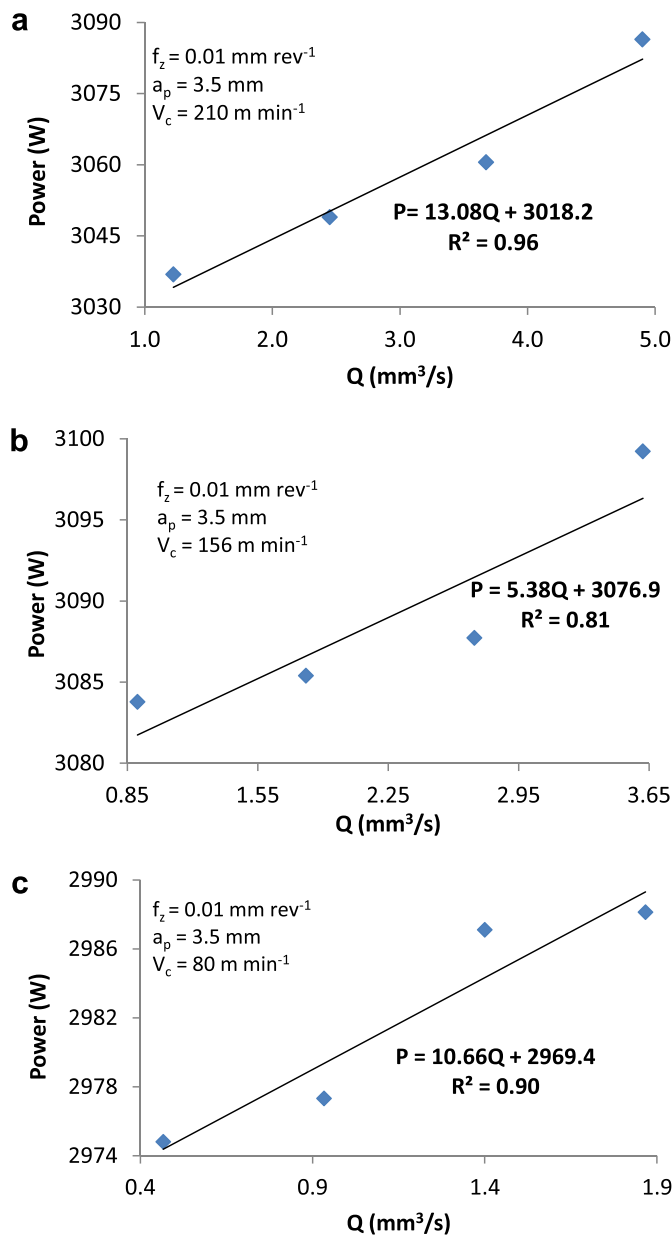


Fig. 2. a: Evaluation of specific cutting energy coefficient at 0.01 mm/tooth for aluminium AW6082-T6 alloy. b: Evaluation of specific cutting energy coefficient at 0.01 mm/tooth for AISI 1045 steel alloy. c: Evaluation of specific cutting energy coefficient at 0.01 mm/tooth for titanium 6Al-4V alloy.

10.66 W s mm^{-3} with R^2 of 0.96, 0.81 and 0.90 for aluminium AW6082-T6 alloy, AISI 1045 steel alloy and titanium 6Al-4V alloy respectively. At this feed per tooth and axial width of cut of 3.5 mm, the average un-deformed chip thickness was evaluated to be 3 μm using Equation (12) (Boothroyd and Knight, 1989). This un-deformed chip thickness and the specific energy values would be used latter to evaluate the dependence of the two.

$$h_{\text{avg}} = \frac{f_z}{\phi_s} \int_0^{\phi_s} \sin \phi d\phi \quad (12)$$

where h_{avg} represents the average un-deformed chip thickness in mm, f_z is the feed in mm/tooth and ϕ is the swept angle in degrees and ϕ_s is the swept angle in radians.

Fig. 3 show the estimated specific cutting energy coefficient at a feed of 0.28 mm/tooth which is equivalent to an average un-deformed chip thickness of 97 μm . It is observed from Fig. 3a,b and c and at the feed of 0.28 mm/tooth that the specific cutting energy as represented by the slope of the graph was 0.78, 1.97 and 2.55 W s mm^{-3} with R^2 of 1.0, 0.96 and 0.94 for aluminium AW6082-T6 alloy, AISI 1045 steel alloy and titanium 6Al-4V alloy respectively. Compared to a feedrate of 0.01 mm/tooth as in Fig. 2, in Fig. 3 the specific cutting energy significantly reduced to values assumed in literature (Kalpakjian and Schmid, 2003). The increase in specific energy for 0.01 mm/tooth compared to 0.28 mm/tooth can be attributable to increased ploughing and less dominant shearing at the lower un-deformed chip thickness. This is expected because the tool edge radius for the new tooth was evaluated to be 0.06 mm. This means machining at 0.01 mm/tooth (3 μm un-deformed chip thickness) is associated with highly negative effective rake angles.

The evaluation of specific energy was conducted for 0.01, 0.10, 0.19, 0.28, 0.37, 0.46 and 0.55 mm/tooth. For the purposes of saving space, the graphs shown are for the lowest, middle and highest feedrates used. The results for the highest feedrate of 0.55 mm/tooth (un-deformed chip thickness of 190 μm) are shown in Fig. 4a,b and c. For this condition, the specific cutting energy coefficient was 0.21, 1.47 and 1.13 with R^2 of 1.0, 0.99 and 0.92 for aluminium AW6082-T6 alloy, AISI 1045 steel alloy and titanium 6Al-4V alloy respectively. The result at the highest feed settings reveals that the specific cutting energy in the shear cutting regime remains fairly constant despite an increase in feedrate.

A summary of the specific energy coefficient obtained from the study is shown in Table 7 for all the feedrates tested.

The specific cutting energy coefficient was plotted against the un-deformed chip thickness as shown in Fig. 5a,b and c. The relationship between specific energy and un-deformed chip thickness can be represented by a power function. The graphs clearly show that the specific energy coefficient in cutting is fairly constant at higher un-deformed chip thickness (typical of roughing operations) but increases exponentially at low (typical of finishing and/or micro-scale machining operations) un-deformed chip thickness. The exponential increase in specific energy at reduced un-deformed chip thickness can be attributable to highly negative rake angles and increased ploughing and friction. The chip thickness to specific energy trend mirrors that in specific cutting force. Table 2 shows specific cutting force model found in literature.

Based on Fig. 5, new specific energy equations were deduced and these are shown as Equations (13)–(15).

$$k_{\text{Al}} = 0.071 * h^{-0.64} \quad (13)$$

$$k_{\text{S}} = 0.900 * h^{-0.33} \quad (14)$$

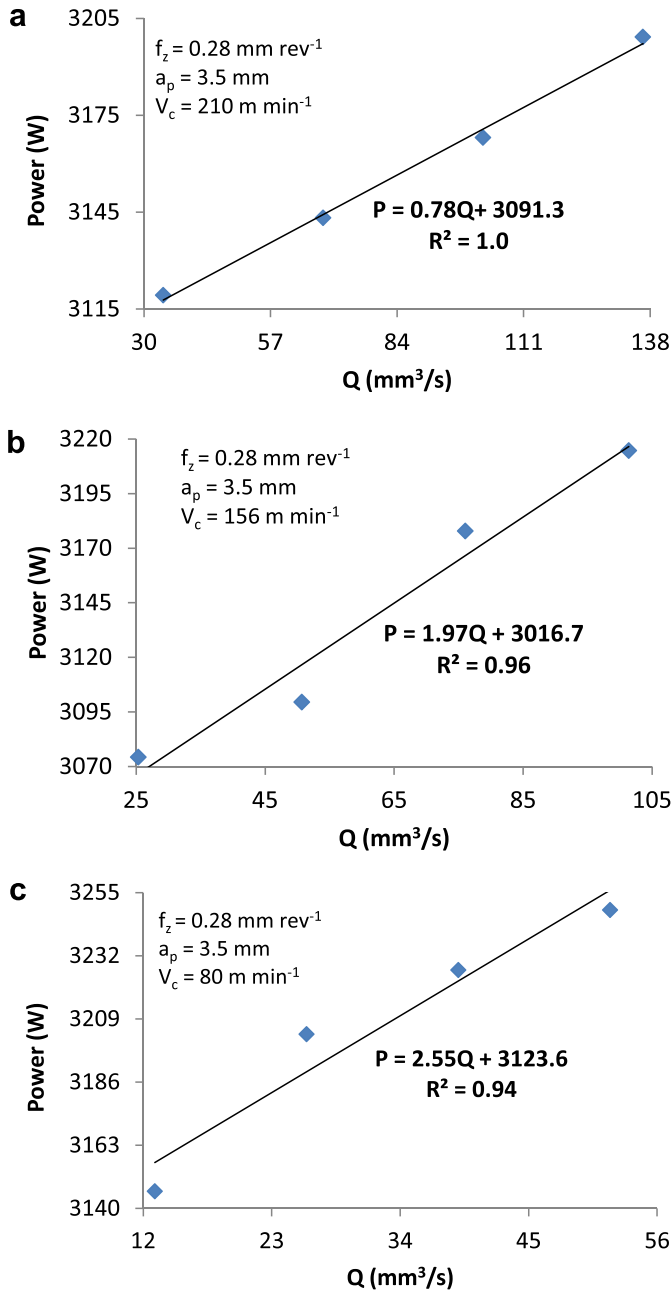


Fig. 3. a: Evaluation of specific cutting energy coefficient at 0.28 mm/tooth for aluminium AW6082-T6 alloy. b: Evaluation of specific cutting energy coefficient at 0.28 mm/tooth for AISI 1045 steel alloy. c: Evaluation of specific cutting energy coefficient at 0.28 mm/tooth for titanium 6Al-4V alloy.

$$k_{Ti} = 0.670 \cdot h^{-0.51} \quad (15)$$

where k_{Al} , k_S and k_{Ti} represents the specific cutting energy in $W \text{ s mm}^{-3}$ of aluminium AW6082-T6 alloy, AISI 1045 steel alloy and titanium 6Al-4V alloy respectively and h is the un-deformed chip thickness in mm.

Fig. 6 compares the specific energy trend for aluminium AW6082-T6 alloy, AISI 1045 steel alloy and titanium 6Al-4V alloy. The variations of specific energy with un-deformed chip thickness for three workpiece materials follow similar power function trend. It is can be seen that aluminium AW6082-T6 alloy specific energy coefficient varies from 13.08 to 0.21 $W \text{ s mm}^{-3}$, and for titanium 6Al-4V alloy the range is 10.66 to 1.13 $W \text{ s mm}^{-3}$ while the range for

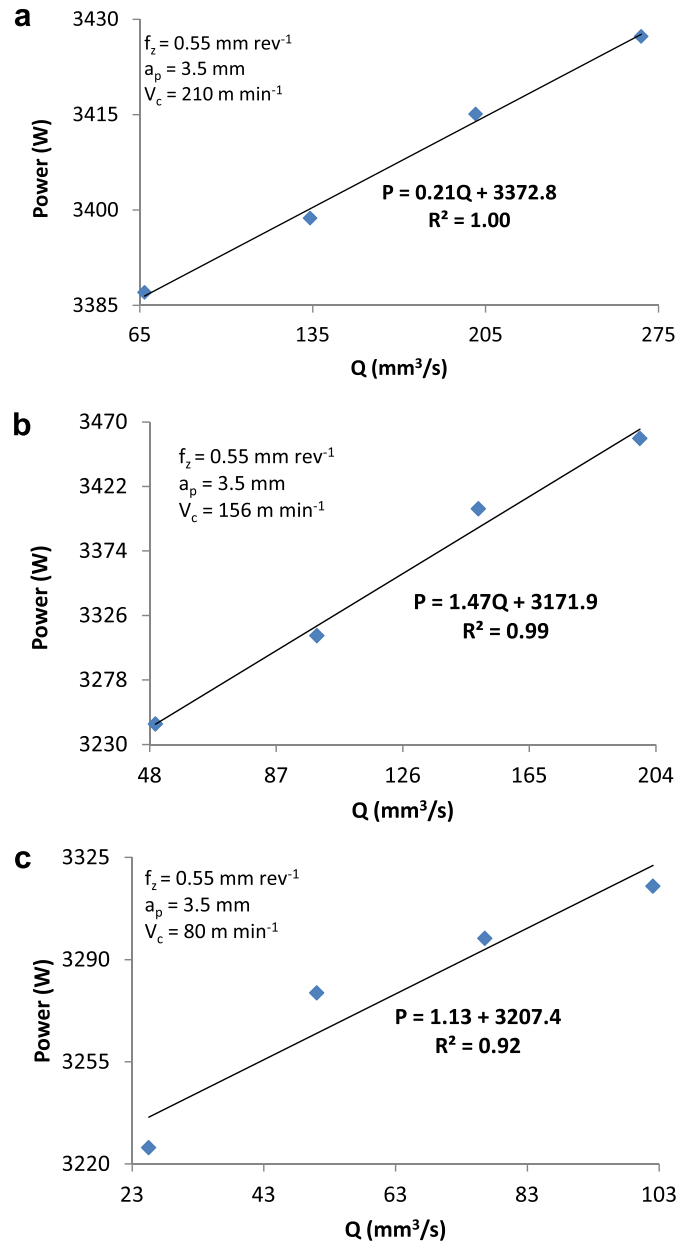


Fig. 4. a: Evaluation of specific cutting energy coefficient at 0.55 mm/tooth for aluminium AW6082-T6 Alloy. b: Evaluation of specific cutting energy coefficient at 0.55 mm/tooth for AISI 1045 steel alloy. c: Evaluation of specific cutting energy coefficient at 0.55 mm/tooth for titanium 6Al-4V alloy.

AISI 1045 steel alloy is 5.38 to 1.47 $W \text{ s mm}^{-3}$. It is observed that for aluminium alloys the specific energy for cutting can be significantly high at very low un-deformed chip thickness to significantly low at chip thicknesses typical of conventional machining.

From the three workpiece materials, it can be concluded that a generic model for the relationship between specific energy and the un-deformed chip thickness can be represented by Equation (16).

$$k_e = K_e h^{-x} \quad (16)$$

where k_e is the specific cutting energy in $W \text{ s mm}^{-3}$ at the required un-deformed chip thickness and K_e is the specific area energy in $W \text{ s mm}^{-2}$ at un-deformed chip thickness of 1 mm, and h is the un-deformed chip thickness in mm while x is the specific energy exponent.

Table 7
Experimental values of *k* at different un-deformed chip thickness *h*.

| Specific cutting energy (Ws mm ⁻³) | Feed, <i>f_z</i> (mm/tooth) <i>h_{avg}</i> (μm) | Data obtained in this study | | | | | | | |
|--|--|-----------------------------|------|------|------|------|------|------|--------------------------------|
| | | 0.01 | 0.10 | 0.19 | 0.28 | 0.37 | 0.46 | 0.55 | Kalpakkjian and Schmid (2003). |
| Aluminium AW6082-T6 Alloy | | 13.08 | 1.99 | 1.52 | 0.78 | 0.87 | 0.21 | 0.21 | 0.40–1.00 |
| AISI 1045 steel alloy | | 5.38 | 3.73 | 2.08 | 1.97 | 1.65 | 1.55 | 1.47 | 2.00–9.00 |
| Titanium alloy | | 10.66 | 4.45 | 3.78 | 2.55 | 2.65 | 1.14 | 1.13 | 2.00–5.00 |

4.1. Specific energy and size effect

The ratio of the un-deformed chip thickness to the cutting edge radius is one of the key measures for defining the size effect in machining. The specific energy was plotted as a function of this

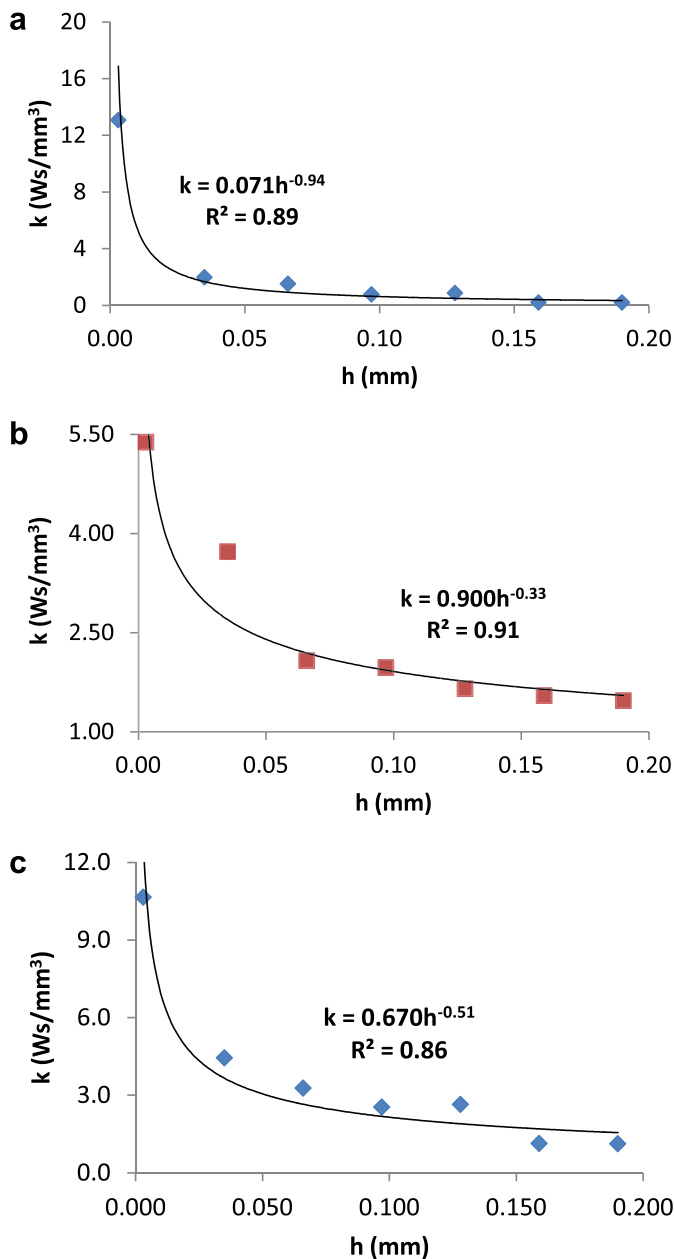


Fig. 5. a: Specific cutting energy model of aluminium AW6082-T6 Alloy. b: Specific cutting energy model of AISI 1045 steel alloy. c: Specific cutting energy model of titanium 6Al-4V alloy.

ratio in order to elucidate the effect of machining length scale on the energy efficiency for material removal. The coefficient of the graphs in Fig. 7a,b and c is equivalent to the specific energy at un-deformed chip thickness equal to tool edge radius. This value is the upper limit for the specific energy experienced in machining when shearing mechanisms instead of ploughing dominate. These experimental values derived are in agreement with mid range values published by Kalpakjian and Schmid (2003). It therefore implies that the empirical modelling adopted is a robust approach for determining the specific cutting energy for various materials. So, from Fig. 7a,b and c, the coefficients of 1.01, 2.26 and 2.78 indicate that aluminium AW6082-T6 alloy has the lowest average specific energy in shear dominated machining followed by AISI 1045 steel alloy and titanium 6Al-4V alloy in increasing order of difficult-to-cut materials. Thus, the tip energy in machining processes and environmental impact of materials processing is influenced by material machinability as driven by workpiece material properties.

5. Conclusions

This research investigated the variation of specific energy coefficient for a wide range of un-deformed chip thicknesses and three different workpiece materials that are widely used in engineering. The specific energy coefficient is a fundamental quantity required for the estimation of tool tip energy and can have impact on surface integrity of machined parts. The following conclusions were drawn as a result of this study:

1. A new generic model for the specific cutting energy coefficient based on the un-deformed chip thickness for aluminium AW6082-T6 alloy, AISI 1045 steel alloy and titanium 6Al-4V alloy has been presented in this work. The model is in agreement with the theory for specific cutting force models. The specific cutting energy can be modelled from the following generic relationship.

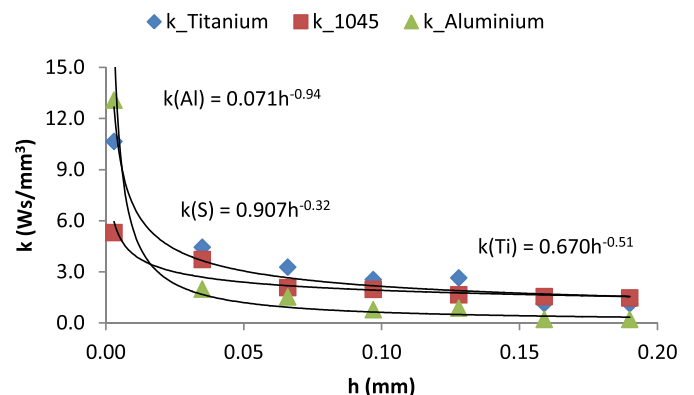


Fig. 6. Specific energy comparison for aluminium AW6082-T6 alloy, AISI 1045 steel alloy and titanium 6Al-4V alloy.

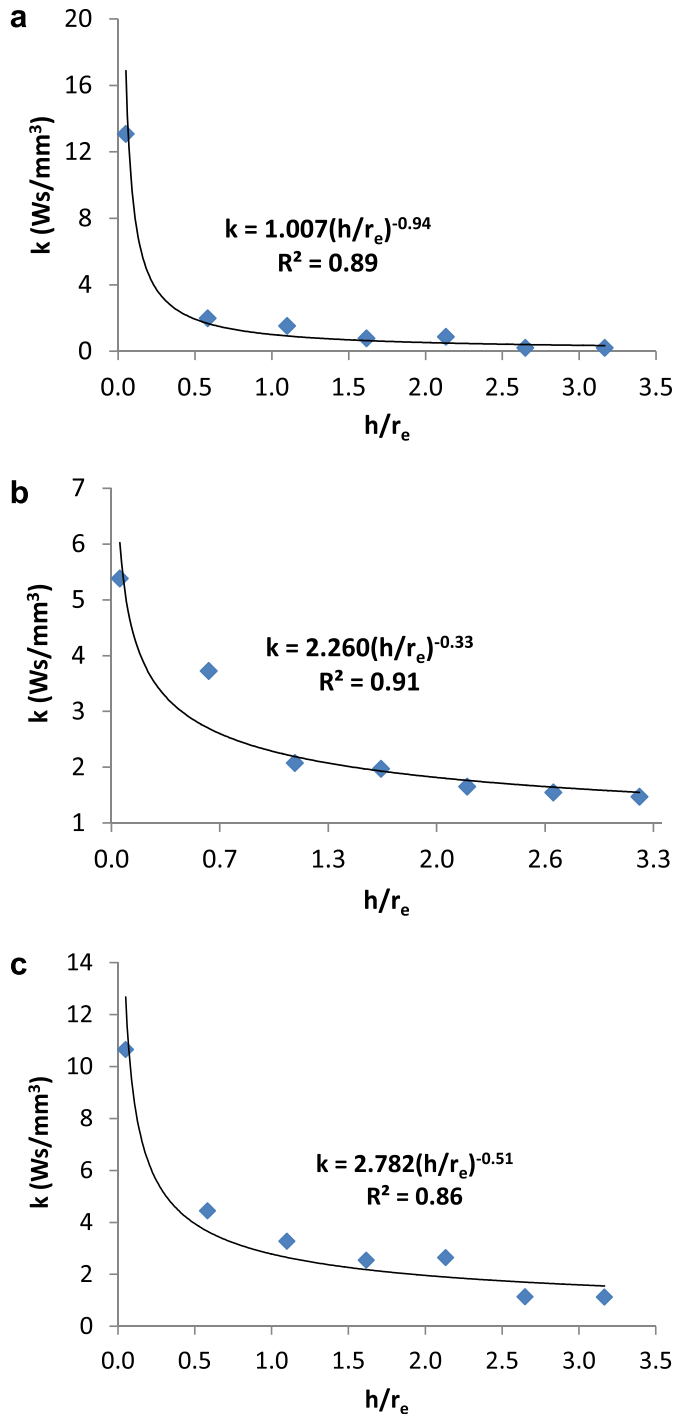


Fig. 7. a: Specific energy size effect in machining of aluminium AW6082-T6 alloy. b: Specific energy size effect in machining of AISI 1045 steel alloy. c: Specific energy size effect in machining titanium 6Al-4V alloy.

$$k_e = K_e h^{-x}$$

where k_e is the specific cutting energy in $W s mm^{-3}$ at the required un-deformed chip thickness and K_e is the specific area energy in $W s mm^{-2}$ at un-deformed chip thickness of 1 mm, and h is the un-deformed chip thickness in mm while x is an experimentally determined specific energy exponent.

2. The variation of specific energy with un-deformed chip thickness for three workpiece materials follows similar power

function trends. For the aluminium AW6082-T6 alloy, specific energy coefficient varies from 13.08 to 0.21 $W s mm^{-3}$, and for titanium 6Al-4V alloy the range is 10.66 to 1.13 $W s mm^{-3}$ while the range for AISI 1045 steel alloy is 5.38 to 1.47 $W s mm^{-3}$.

3. For aluminium alloys the specific energy for cutting can be significantly high at very low un-deformed chip thickness to significantly low at chip thicknesses typical of conventional machining.
4. A representative average value of specific energy for different workpiece materials is evaluated at a condition where the un-deformed chip thickness is equal to the tool edge radius. Since this is the upper limit for the shear dominant mechanism. On this basis the average specific energy in conventional machining for a positive 5° rake angle carbide tool is 1.007, 2.260 and 2.782 $W s mm^{-3}$ for aluminium AW6082-T6 alloy, AISI 1045 steel alloy and titanium alloy respectively.
5. This study shows that the specific energy is significantly influenced by feedrate. To reduce energy consumption during manufacturing it is recommended that bulk material removal (roughing) should be undertaken at feedrates greater than the tool edge radius.
6. This study is based on specific energy evaluation without a focus on modelling impact of tool wear; more research work is needed to investigate the sensitivity of this model to tool wear.
7. Electrical energy demand in manufacturing is a significant contributor to the global warming potential (GWP) and environmental burden of manufacturing industries. Fundamental to evaluating the energy demand is a need for data on specific energy requirements for machining different materials. Thus, the paper contributes key data required for energy demand modelling and energy smart and environmentally friendly manufacturing.

References

- Aramcharoen, A., Mativenga, P., 2009. Size effect and tool geometry in micro milling of tool steel. *Precis. Eng.* 33, 402–407.
- Balogun, V.A., Mativenga, P.T., 2013. Modelling of direct energy requirements in mechanical machining processes. *J. Clean. Prod.* 41, 179–186.
- Bayoumi, A.E., Yucesan, G., Hutton, D.V., 1994. On the closed form mechanistic modelling of milling: specific cutting energy, torque, and power. *J. Mater. Eng. Perform.* 3, 151–158.
- Bissacco, G., Hansen, H.N., De Chiffre, L., 2006. Size effects on surface generation in micro milling of hardened tool steel. *CIRP Ann. Manuf. Tech.* 55, 593–596.
- Boothroyd, G., Knight, W.A., 1989. *Fundamentals of Machining and Machine Tools*. Marcel Dekker, New York.
- Dahmus, J., Gutowski, T., 2004. An environmental analysis of machining. In: *Proc. ASME Inter. Mech. Eng. Congr. R&D Expos*, pp. 13–19.
- Diaz, N., Redelsheimer, E., Dornfeld, D., 2011. Energy consumption Characterization and Reduction Strategies for Milling Machine Tool Use, *Globalized Solutions for Sustainability in Manufacturing*, pp. 263–267.
- Draganescu, F., Gheorghe, M., Doicin, C.V., 2003. Models of machine tool efficiency and specific consumed energy. *J. Mater. Process. Tech.* 141 (1), 9–15.
- Ducobu, F., Filippi, E., Rivière-Lorphèvre, E., 2009. Chip formation and minimum chip thickness in micro-milling. In: *Proceedings of the CIRP Conference on Modelling of Machining Operations*, pp. 339–346.
- Filiz, S., Conley, C.M., Wasserman, M.B., Ozdoganlar, O.B., 2007. An experimental investigation of micro-machinability of copper 101 using tungsten carbide micro-endmills. *Int. J. Mach. Tools Manufact.* 47, 1088–1100.
- Ghosh, S., Chattopadhyay, A., Paul, S., 2008. Modelling of specific energy requirement during high-efficiency deep grinding. *Int. J. Mach. Tools Manufact.* 48, 1242–1253.
- Guo, Y., Loenders, J., Duflou, J., Lauwers, B., 2012. Optimization of energy consumption and surface quality in finish turning. *Procedia CIRP* 1, 512–517.
- Gutowski, T., Dahmus, J., Thiriez, A., 2006. Electrical energy requirements for a manufacturing process. In: *Proceedings of 13th CIRP International Conference on Life Cycle Engineering*, Leuven, p. 623.
- Hucks, 1955. Cutting forces and mechanics of materials. *Ind. Indic.* 77, 365–370 (in German).
- Hu, S., Liu, F., He, Y., Hu, T., 2012. An on-line approach for energy efficiency monitoring of machine tools. *J. Clean. Prod.* 27, 133–140.
- Kalpakjian, S., Schmid, S., 2003. *Manufacturing Processes for Engineering Materials*. Prentice-Hall, Englewood Cliffs, New Jersey.

- Kellens, K., Dewulf, W., Overcash, M., Hauschild, M.Z., Duflou, J.R., 2012. Methodology for systematic analysis and improvement of manufacturing unit process life cycle inventory (UPLCI) CO2PEI Initiative (cooperative effort on process emissions in manufacturing), Part 2: case studies. *Int. J. Life Cycle Assess.* 17 (2), 242–251.
- Kienzle, O., 1952. The determination of forces and services to metal cutting machine tools. *Assoc. Ger. Eng.* 94, 299–305 (in German).
- Kronenberg, 1927. *Basic Course of the Machine Cutting Teachings*. Springer-Verlag, Berlin (in German).
- Kuram, E., Ozcelik, B., Bayramoglu, M., Demirbas, E., Simsek, B.T., 2013. Optimization of cutting fluids and cutting parameters during end milling by using D-optimal design of experiments. *J. Clean. Prod.* 42, 159–166.
- Li, W., Kara, S., 2011. An empirical model for predicting energy consumption of manufacturing processes: a case of turning process. *Proc. Inst. Mech. Eng. Part B J. Eng. Manuf.* 225 (B9), 1636–1646.
- Lin, L., Jihong, Y., Zhongwen, X., 2013. Energy requirements evaluation of milling machines based on thermal equilibrium and empirical modelling. *J. Clean. Prod.* 52, 113–121.
- Lucca, D., Seo, Y., Komanduri, R., 1993. Effect of tool edge geometry on energy dissipation in ultraprecision machining. *CIRP Ann. Manuf. Tech.* 42, 83–86.
- Paul, S., Chattopadhyay, A., 1995. A study of effects of cryo-cooling in grinding. *Int. J. Mach. Tools Manufact.* 35, 109–117.
- Pawade, R.S., Sonawane, H.A., Joshi, S.S., 2009. An analytical model to predict specific shear energy in high-speed turning of Inconel 718. *Int. J. Mach. Tools Manufact.* 49, 979–990.
- Polini, W., Turchetta, S., 2004. Force and specific energy in stone cutting by diamond mill. *Int. J. Mach. Tools Manufact.* 44, 1189–1196.
- Qjilian, W., Fei, L., Congbo, L., 2013. An integrated method for assessing the energy efficiency of machining workshop. *J. Clean. Prod.* 52, 122–133.
- Rajemi, M.F., Mativenga, P.T., Aramcharoen, A., 2010. Sustainable machining: selection of optimum turning conditions based on minimum energy considerations. *J. Clean. Prod.* 18, 1059–1065.
- Sabberwal, A.J.P., 1962. Cutting forces in down milling. *Int. J. Mach. Tool. Des. Res.* 2, 27–41.
- Schroder, H.J., 1934. The importance of small chip thickness in rolling milling cutter. *Mech. Eng. Bus.* 13, 541–548 (in German).
- Zhang, T., Liu, Z., Xu, C., 2013. Influence of size effect on burr formation in micro cutting. *Int. J. Adv. Manuf. Technol.*, 1–7.
- Zhang, T., Liu, Z.Q., Xu, C.H., He, N., Li, L., 2012. Experimental Investigations of Size Effect on Cutting Force, Specific Cutting Energy and Surface Integrity during Micro Cutting. *Materials Science Forum*, pp. 371–376. *Trans Tech Publ.*